JOURNAL OF MATERIALS SCIENCE 25 (1990) 4211–4215

# Fracture toughness of metal reinforced glass composites

G. BARAN
*Temple University School of Dentistry, Philadelphia, Pennsylvania 19140, USA*
M. DEGRANGE
*Laboratory for Biomaterials, University of Paris V, France*
C. ROQUES-CARMES, D. WEHBI
*Laboratory for Surface Microanalysis, Ecole Normale Superieure, Besancon, France*

The effect of hardness and strength of particulate reinforcements on the toughening of a glass matrix composite have been investigated. Spherical particles of two gold-based alloys were blended with a low-fusing glass powder; the mixture was hot-pressed, and disc-shaped specimens prepared for fracture toughness testing using the strength/flaw method. Scanning electron microscopy was used to examine fracture surfaces. It was found that the softer, more ductile alloy was a more effective toughening additive than the harder alloy.

## 1. Introduction

Strengthening and toughening of some ceramics can be achieved by dispersing metal particles within the brittle matrix. Examples of such composite systems include $Al_2O_3$/Mo [1, 2], MgO/Fe, Co, Ni [3], glass/Ni [4], glass/W [5], and $ZrO_2$/Zr [6]. The reported increases in toughness in these systems were small, and attributed to changes in crack direction, or load sharing by the dispersed phase. It was recently claimed that an eight-fold increase in fracture toughness could be achieved through use of oxidized aluminium particles in glass [7]. Important features of that glass/aluminium composite included the match of elastic properties of both phases, and chemical bonding between glass and aluminium. In another system where particle/matrix bonding existed, Moore and Kunz [8] obtained four-fold increases in toughness in a glass/Kovar alloy composite when the alloy was etched to enhance mechanical interlocking with the matrix.

According to a model of ductile reinforcment of brittle matrices proposed by Krstic [9], optimal toughening occurs when the metal reinforcing particles have low strengths. Presumably, such particles are able to undergo stress relief to minimize the effect of mismatches in the thermal expansion behaviour of the matrix and particle. If the matrix surrounding the particles does not fail and the two phases remain strongly bonded, approaching cracks can interact with the dispersed phase. As the crack extends beyond the particle, the ductile metallic phase deforms, and the ligaments formed in the crack wake contribute to composite toughness.

Another analytical model that predicts the amount of toughening due to ligament formation has been presented by Evans and McMeeking [10], wherein three types of bridging behaviour in reinforced ceramic systems are described. The analysis that postulated hard and strong reinforcing particles was found to correlate best with the toughening observed in two cemented carbide systems and a glass/aluminium composite, even though the two metal reinforcing materials (aluminium and cobalt) differ considerably in their properties. Data from other brittle matrix/ductile reinforcement systems are needed to test or verify the assumptions made in this model.

Some uncertainty exists concerning the role of particle ductility and yielding behaviour (before, during, and after crack/particle interaction) in composite toughening. The strain energy release rate, $\Delta G$, during ligament formation is simply defined as

$$\Delta G = f \int_0^{u_c} \sigma(u)\, du$$

where $f$ is the area of reinforcements intersected by the crack front, $u$ the crack opening, $\sigma$ the stress acting on the ligament, and $u_c$ the critical crack opening. The correlation of $u_c$ with a non-constrained particle ductility (as defined, for example, by the per cent elongation) may be felt intuitively, but the exact relationship between the two properties is difficult to ascertain. This is partly the result of matrix constraints that prevent the particle from achieving the degree of plastic flow suggested by uniaxial tensile testing data. In fact, in cases where the particles of the reinforcing phase are obtained by techniques that differ from the usual bulk manufacturing methods, it is difficult to know which bulk properties remain valid for the particulate form, where porosity and microstructure have a concentrated influence. From Evans and McMeeking [10], one also obtains an estimate of $u$ that is inversely dependent on yield strength, and the general result that toughness increases with the strength ($S$), size, ($R$), and volume fraction ($F$) of the reinforcing phase. The effect of thermal or elastic property mismatch on the direction of crack

0022–2461/90 $03.00 + .12 

propagation is not considered in this model, although the area of reinforcing phase actually encountered by propagating cracks depends very much on the distribution of the elastic stress fields with magnitudes approximated by Selsing's equation [11]. The signs of these fields can cause crack deflection, so that the effective $F$ is different from the assumed $F$.

The desirability of high $S$ particles would also seem to be mitigated by concerns related to particle stress relief and matrix failure prior to particle yielding, particularly in cases when $\alpha_{particle} > \alpha_{matrix}$, where $\alpha$ is the thermal expansion/contraction coefficient.

These apparently conflicting requirements for strength properties of particulate reinforcements, and the confusion regarding use of parameters such as yield strength and ductility in predicting composite performance, prompted the choice of a system for study where the ductility and strength of the reinforcing particles could be varied. In this manner, an appreciation of the significance of these mechanical properties could be obtained.

## 2. Methods and materials

### 2.1. Sample preparation

Two alloys with certain desirable mechanical and chemical properties, described in Table I, were chosen for this study. Both alloys contain indium, an element which forms an adherent oxide layer on the alloy surface, and facilitates chemical bonding between metal and glass. The Y-3 alloy (87 wt % Au, 8% Pt, with Pd, Ag, In, Sn, Fe and Ta) is commercially used for porcelain fused to metal dental restorations, and has a history of performing well in that application. The Au–4In (6 wt % Au, 4% In) alloy was found to bond well to glass in preliminary screening tests done at the outset of this study. Both alloys were obtained from the same manufacturer (Williams Gold and Refining Company, Buffalo, New York) as spherical atomized powder, $-325$ mesh, and were made in the same way. The selection of the matrix glass was based on its low $T_g$, which facilitated hot-pressing, and on its thermal expansion behaviour, which was similar to that of the two alloys. The composition of the glass (Frit P 2V25, Mobay Chemical Corp., Baltimore, Maryland), $Na_2O$–$CaO$–$B_2O_3$–$SiO_2$–$NaF$ (NCBSF), was not considered to be a significant variable. The composites that were eventually made contained 35 vol % reinforcing phase, an amount that provided an average interparticle spacing of $< 50\,\mu m$.

In order to effect bonding between matrix and dispersed phase, the alloy powders were oxidized in air for 15 min at 800° C. Weighed quantities of the alloy and glass powders were dry mixed for 3 h, then pressed at 800° C at an air pressure of $5.3 \times 10^{-6}$ MPa. Dies for hot pressing were made of high-density graphite or a proprietary ceramic investment material (Symphyse Ceramic Investment, Marseille, France). A pressure of 1 MPa was applied uniaxially to aid densification.

### 2.2. Sample preparation and evaluation

Samples obtained by this procedure were cylinders with a length of 20 mm and a diameter of 13 mm. After exterior surfaces were cleaned of debris, composite density was measured by immersion, and the sonic method used to determine Young's modulus and Poisson's ratio. Subsequently, a diamond saw was used to prepare disc-shaped specimens with a thickness of about 1 mm. The flat surfaces of the discs were polished in oil through a 0.33 $\mu$m finish, then given a stress relief anneal for 15 min at 425° C.

Mechanical testing was done with a biaxial flexure apparatus described by Wachtman *et al.* [12]. To obtain values of $K_{Ic}$, a flaw was introduced in the centre of what was to be the tensile face of each specimen using a Vickers indentor under a load of 2.94 N. This load had been found previously to produce well-defined cracks in NCBSF glass. Because controlled flaw techniques have seen only limited use in fracture toughness evaluations of multiphase materials, it was decided to introduce deliberately the flaw into the glassy matrix and thereby maintain control of the flaw size. In this manner, an "effective" $K_{Ic}$ could be calculated [13, 14]. Random placement of the indentation would lead to variations in crack size, as some indentations would fall on a metal particle. Immediately after the flaw was introduced, a drop of oil was placed on that surface.

Specimens were tested by stressing to failure at a displacement rate of 0.1 mm min$^{-1}$. Calculation of $K_{Ic}$ (eff) followed according to the method of Chantikul *et al.* [14].

## 3. Results and discussion

Figs 1 and 2 depict cross-sections through oxidized particles of Y-3 alloy and Au–4In alloy, respectively. The particles are shown to be porous and there appears to be some evidence of internal oxidation. The two-phase structure of Au–4In alloy shown in Figs 2a and b was found to be the result of indium segregation on the rim of the particles, as shown on the indium concentration map of Fig. 2c obtained by energy dispersive analysis of X-rays (EDAX).

TABLE I

| | $E$ (GPa) | $\alpha$ ($10^{-6}$ °C$^{-1}$) | Hardness | | Strength (MPa) | | Elongation (%) | $\nu$ |
|---|---|---|---|---|---|---|---|---|
| | | | KHN | DPH | UTS | YS (0.1%) | | |
| NCBSF Glass | 89* | 12.8* | – | 650* | 49§ | – | – | 0.28* |
| Y-3 | 64.1† | 14.9† | 177* | 165†, 148* | 470† | 330† | 12† | 0.33‡ |
| Au-4In | 73.1‡ | 14.8‡ | 71* | 84* | 103‡ | – | 30‡ | 0.33‡ |

*Measured during this study.
†Measured on cast ingot prior to atomization.
‡Estimated from handbook data.
§Modulus of rupture, biaxial flexure method.

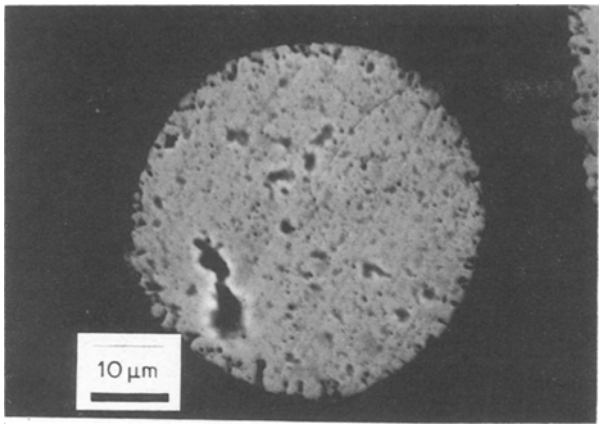


*Figure 1* Electron microscope image of Y-3 alloy particle.

The hardness readings listed in Table I were taken from similar particles after composite specimens had been fabricated. A load of 2 g was used with both Knoop and Vickers indentors. The Knoop geometry is generally more reliable at light loads, as the shallow indentation reduces the anvil effect of the surrounding matrix. Indentations ranged between 10 and 20 $\mu$m in length for the Knoop and 4 to 7 $\mu$m for the Vickers indentors. Although there is no exact correlation between the Vickers or Knoop hardness and material strength, it is generally accepted that Brinell hardness and ultimate tensile strength are related through various constants. We assume here that qualitatively a similar relationship exists between microhardness readings and the strength of the dispersed phase. Chemical analysis indicated that the interior of the Au–4In particles is essentially indium-free. Hardness and composition data therefore both support the view that the Au–4In alloy is considerably softer, more ductile, and weaker than alloy Y-3. The two systems studied here are therefore well suited for determining the influence of yielding behaviour in reinforcing phases on composite toughening.

Figs 3 and 4 depict fracture behaviour of Y-3/glass and Au–4In/glass composites. In Figs 3a and 4a the crack is seen to propagate primarily through the matrix phase, at times avoiding the dispersed alloy particles. Figs 3b and 4b show fracture surfaces, and in Figs 3c and 4c evidence of ductile failure in particles is visible.

Figs 3a and 4a indicate that cracks are deflected while propagating through the glass/metal composite. It is useful to compare the magnitude of toughening observed here with the amount predicted for various toughening mechanisms dependent on crack path modification. Such predictive models are available for crack deflection [15, 16], and crack bowing [17]. The results obtained for those models are summarized in Table II together with our experimental data for $K_{Ic}^{eff}$, representing the mean of ten specimens.

The data indicate that crack deflection models alone do not account for the total toughening observed here. Values of $\sigma_t$ and $\sigma_r$, the tangential and radial stresses around alloy particles obtained from Selsing's equation, are similar for both glass/metal composites. Therefore, the effects of stress fields on crack propagation directions should be similar in both composites. The difference in toughening between the two composites is then due to the difference in physical properties of Y-3 and Au–4In alloys.

Although the predictions of the crack bowing model more closely correspond to the measurements made here, a necessary consequence of that model is that strong obstacles toughen more effectively than weak ones. The results obtained here contradict that prediction, with the weaker Au–4In alloy proving to be more effective than the stronger Y-3 alloy.

The available experimental data on glass/metal composite systems are summarized in Table III. The results of those studies [7, 8, 18] show that greater toughening is possible than was achieved with the glass/gold alloy composites studied here. Exact comparisons are not useful, as little similarity exists between metallic particle sizes and geometry in the various composite systems. Furthermore, the methods used to obtain toughening data or to estimate physical properties varied widely among the studies.

The toughening mechanisms responsible for the effects presented in Table III differ with the particular systems under study. For the case of glass reinforced with Kovar, ligament formation and crack bridging was not relevant even though metal particles were mechanically interlocked with the matrix. Toughening was ascribed to load sharing and crack deflection. The composite containing dispersed niobium metal fibres also showed no evidence of ligament formation, although it was claimed that the fibres were capable of plastic deformation. In fact, no bond between matrix and fibre was demonstrated, and the mechanical

TABLE II

| | $K_{Ic}^{eff}$ | $\sigma_t^*$ | $\sigma_r^*$ | Toughening | | | |
|---|---|---|---|---|---|---|---|
| | | | | Measured $K_{Ic}^{eff}/K_{Ic}^{m}$ | Predicted | | |
| | | | | | Crack deflection | | Crack pinning |
| | | | | | $K_c/K_c^m$ [16] | $G_c/G_c^m$ [15] | $K_c/K_c^0$ [17] |
| NCBSF Glass | 0.63 | – | – | – | – | – | – |
| Glass/Y-3 | 1.16 | −27.3 | 54.6 | 1.84 | 1.2–1.8 | 1.7†, 1.35‡, 1.18§ | 2.23¶ |
| Glass/Au–4In | 1.34 | −27.4 | 54.8 | 2.13 | 1.2–1.8 | 1.7†, 1.35‡, 1.18§ | 2.23¶ |

*From Selsing [11], where $\sigma_t$ and $\sigma_r$ are tangential and radial stresses, respectively, and a negative sign indicates compression.
† Distributed particle spacing.
‡ Uniform particle spacing.
§ Increase in surface area of crack.
¶ Weak obstacles.

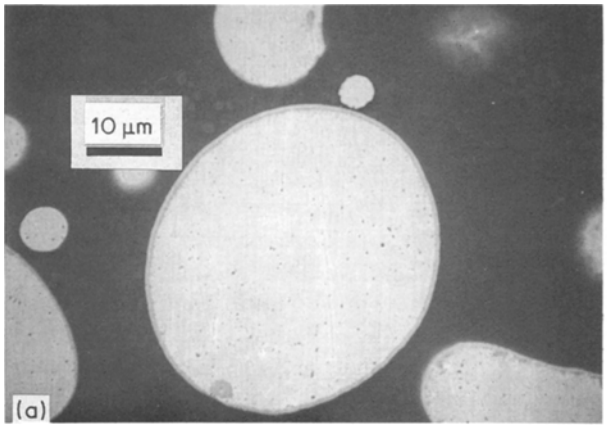


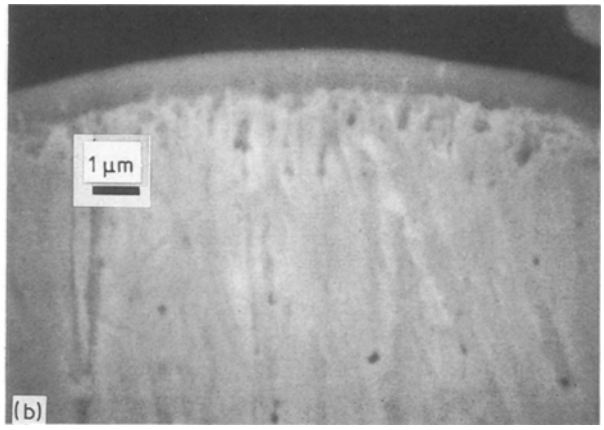


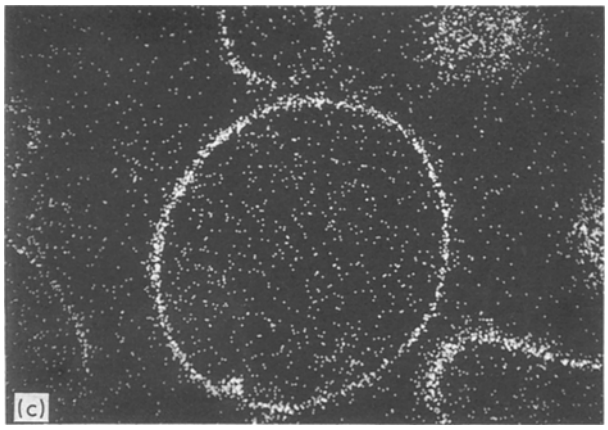


*Figure 2* Electron, reflected light microscope, and element map images of Au–4In alloy particles.

properties of the niobium fibres were not determined. This latter point is significant inasmuch as these properties are strongly dependent on processing history.

Toughening achieved in the aluminium/glass system described in Table III [7] is remarkably high, and was not satisfactorily predicted by the theory presented in the original investigation. Some success was later achieved by a treatment that regarded aluminium particles to be "strong" reinforcements, but no property testing of the aluminium particles was performed [15]. Nonetheless, when comparing the results obtained with Kovar, niobium, and aluminium dispersions, it is significant to note that the greatest amount of toughening was achieved in the system containing a ductile reinforcement.

Results obtained in the study here indicate that in cases where similar thermal and elastic stresses surround reinforcing particles of different strengths, particles with greater ductility and a lower yield strength provide greater toughening. In the light of this evidence and the data cited by others, a satisfactory explanation for the exceptional toughening effects of aluminium particles in glass is difficult to find.

In order to ascertain empirically the toughening ability of ductile ligaments, it would be useful to identify a brittle matrix/ductile particle system where propagating cracks encounter all nearest neighbour reinforcements.

## Acknowledgements

The authors thank Mr Rigondaud and Mr Tetard, CNRS Laboratory for New Ceramics, Limoges,

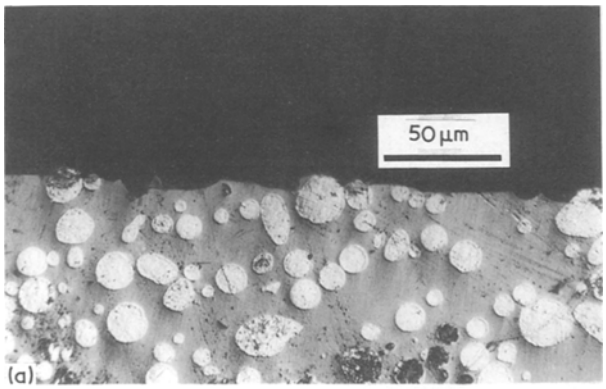


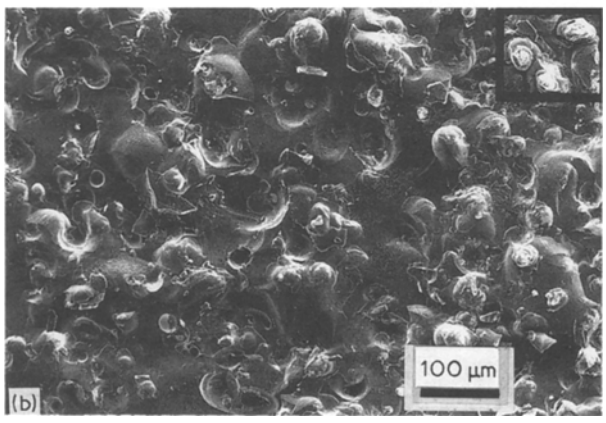


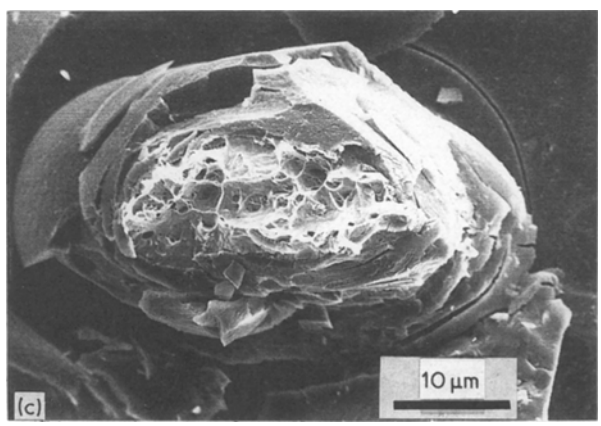


*Figure 3* Fractured surfaces and edges of Y-3 alloy/glass composite.

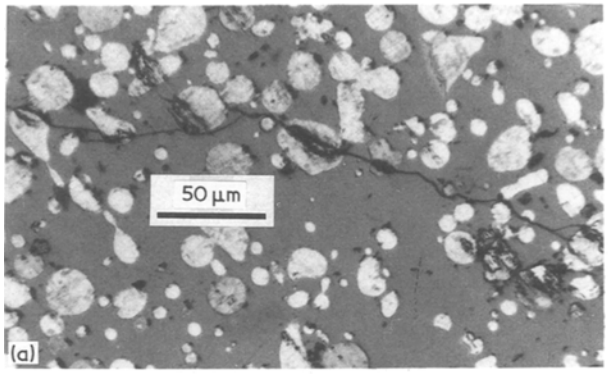


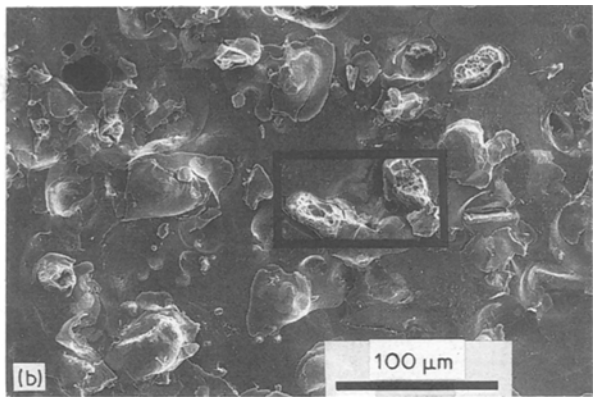


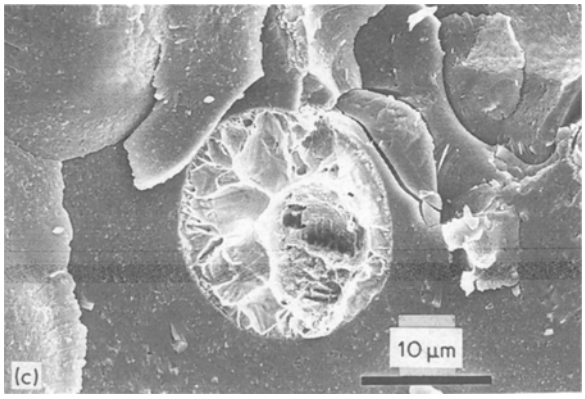


*Figure 4* Fractured surfaces and edges of Au–4In alloy/glass composite.

TABLE III

| Metallic phase | Toughening ($K_c/K_c^m$) |
|---|---|
| Au–Pt, Pd | 1.84* |
| Au–4 In | 2.13* |
| Kovar | 3.82† |
| Nb | 3.0‡ |
| Al | 8.1§ |

*35 vol %, spherical, −325 mesh.
†25 vol %, spherical, −200, +325 mesh [8].
‡30 vol % fibre, 1 to 4 μm diameter, 10 to 50 μm long [18].
§20 vol %, irregular spherical, −120, +140 mesh [7].

France, for assistance in sample preparation, Dr Abouaf, School of Mines of Paris, Corbeilles, France, for assistance with sonic measurement techniques, Dr Sadoun, Laboratory for Synthesis and Study of Microstructures, Paris, for assistance with sample preparation and testing, Mr Chris Johnson, National Bureau of Standards, Gaithersburg, USA, for assistance with microhardness measurements. The National Institutes of Health are thanked for their support of one of us (G. Baran) as a Senior Fellow on research leave, and Temple University for partial support of this research.

## References

1. C. O. McHUGH, T. J. WHALEN and M. HUMENIK Jr, *J. Amer. Ceram. Soc.* **49** (1966) 486.
2. D. T. RANKIN, J. J. STIGLICH, D. R. PETRAK and R. RUH, *ibid.* **54** (1971) 277.
3. P. HING and G. W. GROVES, *J. Mater. Sci.* **7** (1972) 427.
4. M. A. STETT and R. FULRATH, *J. Amer. Ceram. Soc.* **51** (1968) 599.
5. Y. NIVAS and R. M. FULRATH, *ibid.* **53** (1970) 188.
6. A. V. VIRKAN and D. L. JOHNSON, *ibid.* **60** (1977) 514.
7. V. D. KRSTIC, P. S. NICHOLSON and R. G. HOAGLAND, *ibid.* **64** (1981) 499.
8. R. H. MOORE and S. C. KUNZ, *Ceram. Engng Sci. Proc.* **8** (1987) 839.
9. V. D. KRSTIC, *Phil. Mag. A* **48** (1983) 695.
10. A. G. EVANS and R. M. McMEEKING, *Acta Metall.* **34** (1986) 2435.
11. J. SELSING, *J. Amer. Ceram. Soc.* **44** (1961) 419.
12. J. B. WACHTMAN Jr, W. CAPPS and J. MANDEL, *J. Mater.* **7** (1972) 188.
13. R. F. COOK, S. W. FREIMAN and T. L. BAKER, *Mater. Sci. Engng* **77** (1986) 199.
14. P. CHANTIKUL, G. R. ANSTIS, B. R. LAWN and D. B. MARSHALL, *J. Amer. Ceram. Soc.* **64** (1981) 539.
15. K. T. FABER and A. G. EVANS, *Acta Metall.* **31** (1983) 565.
16. S. G. SESHADRI, M. SRINIVASAN and K. M. KEELER, *Ceram. Engng Sci. Proc.* **8** (1987) 671.
17. D. J. GREEN, P. S. NICHOLSON and J. D. EMBURY, *J. Amer. Ceram. Soc.* **66** (1983) C4.
18. J. P. LUCAS, L. E. TOTH and W. W. GERBERICH, *ibid.* **63** (1980) 280.
19. T. L. JESSEN, J. J. MECHOLSKY and R. H. MOORE, *Amer. Ceram. Soc. Bull.* **65** (1986) 377.

*Received 11 April*
*and accepted 16 August 1989*